Critical and oscillatory behavior of a system of smart preys and predators

Alejandro F. Rozenfeld* and Ezequiel V. Albano[†]

Instituto de Investigaciones Fisicoquímicas Teóricas y Aplicadas (INIFTA), Facultad de Ciencias Exactas, UNLP, CONICET, CIC, Sucursal 4, Casilla de Correo 16, (1900) La Plata, Argentina

It is shown that a system of smart preys and predators exhibits irreversible phase transitions between a regime of prey-predator coexistence and an state where predator extinction is observed. Within the coexistence regime, the system exhibits a transition between a regime where the densities of species remain constant and another with self-sustained oscillations, respectively. This transition is located by means of a combined treatment involving finite-size scaling and Fourier transforms. Furthermore, it is shown that the transition can be rationalized in terms of the standard percolation theory. The existence of an oscillatory regime in the thermodynamic limit, which is in contrast to previous findings of Boccara *et al.* [Phys. Rev. E **50**, 4531 (1994)], may be due to subtle differences between the studied models.

I. INTRODUCTION

The understanding of far from equilibrium irreversible dynamical systems with many degrees of freedom is a topic of great interest in many branches of science such as Physics, Biology, Sociology, Economy, Chemistry, Ecology, etc. Within this context, very recently, the study of cooperative phenomena in multicomponent systems of biological and ecological interest has been addressed by physicists using powerful and well-established techniques already developed in the fields of condensed matter physics, statistical physics, and computational physics [1–3].

Some of these studies were aimed to describe, e.g., the formation and development of complex spatiotemporal structures involving cell cultures [4], living organisms ranging from primitive ones such as bacteria [5], fungi colonies [6], and swarms of insects to more sophisticated species such as herds of wildebeest, schools of fish, flocks of birds [7], etc. Within this context the classical Lotka-Volterra (LV) [8] approach is the archetype model for the description of a two-species competition system such as in the case of preys and predators. The main result of the standard mean-field approach for the LV model is the occurrence of oscillatory behavior of population densities with a well-determined period. Natural populations of plants and animals frequently exhibit various patterns of fluctuations about long-term periods [9]. Some species have roughly a constant population density while others exhibit large fluctuations with cyclic or quasicyclic behavior. These deviations from the mean-field predictions may be due to the stochastic nature of the system or, on the other hand, could correspond to chaotic behavior. Very recently, it has been shown that adding a noise term to the equation of a symmetric two-species composition LV model, one could drastically change its behavior. An interesting effect is, e.g., the observation of stochastic resonance [10].

In the present work we study a lattice gas model for a prey-predator system with smart pursuit and escape, which is a variant of the cellular-automata early proposed by Boccara *et al.* [11]. The main finding of the present work is the occurrence of a transition between a regime where the density of species remains constant and another where it exhibit self-sustained oscillations, respectively. In order to identify this transition we have developed a combined treatment involving finite-size scaling and Fourier analysis. It is also shown that the transition can be rationalized in terms of the standard percolation theory.

II. DESCRIPTION OF THE MODEL

The prey-predator model with smart pursuit and evasion is defined as follows: a lattice site can be either empty or occupied by a prey or a predator, respectively. Double occupancy of sites is forbidden. The system evolves according to consecutive cycles: (i) coexistence of species and (ii) escape-pursuit dynamics.

The rules of coexistence are as follows. (a) Preys give an offspring occupying an empty next neighbor site with probability B_H (birth probability of preys) in case of absence of predators within their V_H (visual range of preys). (b) Predators can eat a prey that exist in their M_P (movement range of predators) with probability D_H (death probability of preys). (c) Predators that previously have eaten a prey can give an offspring in the site occupied previously by the eaten prey, with probability B_P (birth probability of predators). (d) Predators can suddenly die with probability D_P (death probability of predators).

In order to formulate the rules for a smart escape-pursuit process we have to note that predators (preys) can feel the presence of an attractive (repulsive) potential $g_{P,H}$ ($g_{H,P}$) generated by the density of preys (predators) in their V_P (V_H) respectively. Furthermore, they are able to calculate the gradient of this potential in their M_P (M_H), namely,

$$g_{a,b}(\vec{\mathcal{X}},t) = \sum_{\vec{\mathcal{X}}' \,\epsilon[V_a \cap E_b(t)]} |\vec{\mathcal{X}} - \vec{\mathcal{X}}'|^{-1}, \qquad (1)$$

────────

*FAX: 0054-221-4254642.

Email address: aleroz@cyrrus.inifta.unlp.edu.ar

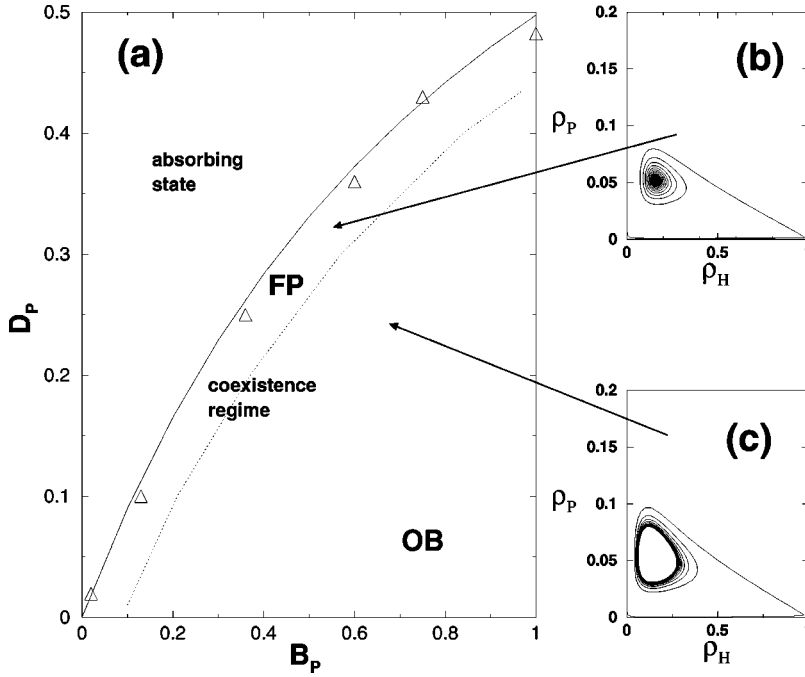[†]Email address: ealbano@inifta.unlp.edu.ar

FIG. 1. (a) Plot of the critical points of the irreversible phase transition between the coexistence regime of prey and predators and the absorbing state with predator extinction. ''Full line '' mean-field results obtained using Eq. (5). △ results from Monte Carlo epidemic studies. ''Dashed line'' critical curve at the fixed point (FP) - oscillatory behavior (OB) transition obtained by means of Monte Carlo simulations (mean-field calculations), respectively. (b) and (c) are plots of predator density versus prey density showing the FP and OB regimes, respectively. Densities are measured in units of number of species per unit area.

where $\vec{\mathcal{X}}$ points to the possible next selected position, $\vec{\mathcal{X}}'$ runs through the subspace occupied by the species b inside the visual space of the species a, V_a is the visual range of the species a, and E_b is the total space occupied by the species b.

Based on these definitions we formulate the escape-pursuit rules as follows.

(a) Preys move into an empty site in the direction of the calculated gradient, the new selected position $\vec{\mathcal{X}}^*$ minimizes the potential $g_{H,P}$ in M_H, $\vec{\mathcal{X}}^* = \text{Arg Min}_{\vec{\mathcal{X}} \epsilon [M_P \cap E_0(t)]} g_{H,P}$ $(\vec{\mathcal{X}}, t)$.

(b) Predators move into an empty site in the direction of the gradient, the new selected position $\vec{\mathcal{X}}^*$ maximizes the potential $g_{P,H}$ in M_P, $\vec{\mathcal{X}}^* = \text{Arg Max}_{\vec{\mathcal{X}} \epsilon [M_P \cap E_0(t)]} g_{P,H}$ $(\vec{\mathcal{X}}, t)$.

In this context, if we define the spatiotemporal density of the species ''s'' as

$$\rho_s(\vec{\mathcal{X}}, t) = \begin{cases} \dfrac{1}{N_s(t)}, & \text{if } \vec{\mathcal{X}} \epsilon E_s \\ 0, & \text{otherwise,} \end{cases} \quad (2)$$

then $g_{a,b}(\vec{\mathcal{X}}, t) = \Sigma_{\vec{\mathcal{X}}' \epsilon V_a} |\vec{\mathcal{X}} - \vec{\mathcal{X}}'|^{-1} \rho_b(\vec{\mathcal{X}}', t)$ and the existence of a force inversely proportional to the squared distance becomes evident. It should be noted that this kind of repulsion-attraction forces between animals have already been used for the theoretical study of the collective motion of self-driven individuals [12].

We have restricted ourselves to investigate the dependence of the system on the predator birth (B_P) and death (D_P) probabilities, respectively. The remaining parameters are kept constant, namely, $M_P = V_P = V_H = 1$. The model is studied by means of Monte Carlo simulations on the square

lattice of side L, measured in lattice units (L.U.) with periodic boundary conditions. During a Monte Carlo time step (mcs) all sites of the sample are update once on average. The model is also studied using a set of mean-field equations. In this case the time is measured in arbitrary units.

III. RESULT AND DISCUSSION

Starting from a random distribution of prey and predators, the system may evolve towards two different states or phases [see Fig. 1(a)]: i) For $D_P \to 0$ (but $D_P > 0$) and $B_P \to 1$ (but $B_P < 1$), the final state of the system is a stationary regime with coexistence of preys and predators [13]; ii) For $D_P \to 0.5$ and $B_P \to 0$ (but $B_P > 0$), predators die out and surviving preys cover the whole lattice. This phase is an absorbing state where the system becomes irreversibly trapped since the spontaneous birth of predators is not allowed. At the boundary between these two phases a critical curve in the $[D_P, B_P]$ plane can be located.

It is well known that the determination of the critical points and critical exponents characterizing irreversible phase transitions (IPT's) using simulations of the stationary state in finite lattices is heavily hindered by fluctuations effects that may irreversibly drive the system into the absorbing state. In order to overcome this difficulty we have performed standard epidemic studies [14]. Starting from a configuration very close to the absorbing state, namely, a lattice covered by preys except by one predator in the center of the sample, the dynamics of the predator's spreading is followed as a function of time measuring (i) the average number of predators $N_P(t)$, (ii) the survival probability of predators, namely, the probability that at time t there is still a predator alive, $P_P(t)$, and (iii) the average spreading distance $R^2(t)$. At criticality, these quantities obey power law behavior, i.e., $N_P(t) \sim t^\eta$, $P_P(t) \sim t^{-\delta}$, and $R^2(t) \sim t^z$. Using this technique we have precisely determined the critical

points shown in Fig. 1(a) and for the critical exponents we get $\eta \approx 0.21 \pm 0.02$, $\delta \approx 0.45 \pm 0.02$, and $z \approx 1.12 \pm 0.02$. So, the second order IPT's between the coexistence regime and the absorbing state can be placed within the universality class of directed percolation, with $\eta = 0.214 \pm 0.008$, $\delta \approx 0.460 \pm 0.006$, and $z \approx 1.134 \pm 0.004$ [14].

The mean-field equations for the system can be derived considering all events causing changes in the population density of both species. So, one has

$$\frac{\partial \rho_P}{\partial t} = \rho_P (B - D), \tag{3}$$

$$\frac{\partial \rho_H}{\partial t} = \rho_H \{ A - (B + C) [1 - (1 - \rho_P)^{(2M_P + 1)^2 - 1}] \}, \tag{4}$$

where ρ_P and ρ_H are the predator and prey densities, respectively. $A = B_H (1 - D_P)^{(2V_H + 1)^2 - 1} [1 - (\rho_P + \rho_H)^8]$ is the birth probability of a prey in a neighboring empty site [15], $B = (1 - D_P) B_P D_H [1 - (1 - \rho_H)^{(2M_P + 1)^2 - 1}]$ is the probability of a predator to catch a prey and have an offspring in the site previously occupied by the prey, $C = (1 - D_P)(1 - B_P) D_H [1 - (1 - \rho_H)^{(2M_P + 1)^2 - 1}]$ is the probability of a predator to catch a prey, and $D = D_P$ is simply the dying probability of a predator. Solving Eqs. (3) and (4), requiring $\partial \rho_P / \partial t = \partial \rho_H / \partial t = 0$ at the critical edge we get

$$B_P^* = \frac{D_P}{D_H (1 - D_P)}. \tag{5}$$

The location of the critical edge using Eq. (5) is also shown in Fig. 1(a) for the sake of comparison with Monte Carlo results. The observed agreement is (surprisingly) excellent considering that in most cases the mean-field approach fails close to second-order transitions. This agreement could be due to the fact that the high density of preys close to the critical point almost inhibits the displacement of predators.

Solving numerically the set of mean-field equations we observed that close to the IPT's critical edge and after a short transient period, the system reaches a constant density of both preys and predators, as is shown in Fig. 2. So, plots of ρ_P versus ρ_H show closed loops ending in a fixed point (FP) as is shown in Fig. 1(b). Within the FP regime [see Fig. 1(a)] the density of predators (preys) steadily increases (decreases) upon increasing B_P. This behavior is also observed in Monte Carlo simulations. However, it should be noticed that within this FP regime preys are the majority species and clusters of preys always percolate across both directions of the sample as, e.g., is shown in the snapshot configuration of Fig. 3. Moving away from criticality, when B_P is further increased, the system starts to exhibit a self-sustained oscillatory behavior (OB) with a well-defined period (see Fig. 1). Therefore a curve can be drawn at the boundary between the FP and OB as is shown in Fig. 1(a).

The location of the boundary between FP and OB regimes using Monte Carlo simulations deserves a careful task. In fact, due to the stochastic nature of the simulation procedure
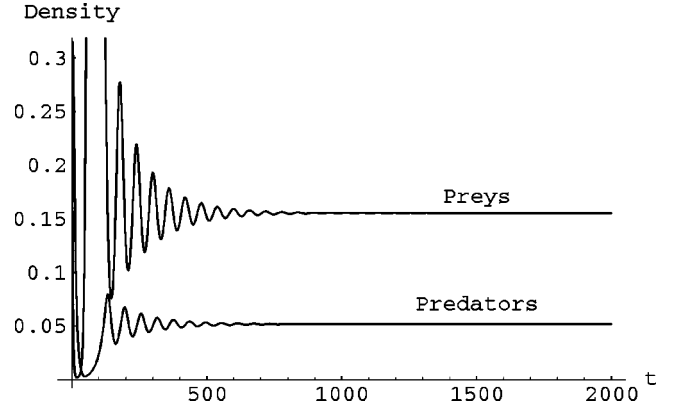

FIG. 2. Plots of the density of prey and predators, measured in units of number of species per unit area, versus time, measured in arbitrary units, as obtained solving the mean-field equations for $D_P = 0.25$ and $B_P = 0.45$. The attainment of the FP regime after a short transient regime can be observed.

one always observes a quasiperiodical signal as is shown in Fig. 4. This quasioscillatory behavior could be, on the one hand, a finite-size effect whose amplitude A_P vanishes in the thermodynamic limit or, on the other hand, simply noise. In order to clarify these points we have first performed a finite size analysis. It is found that the amplitude of the oscillations behaves as $A_P = A_\infty + BL^{-\gamma}$ where B is a constant, A_∞ is the amplitude in the thermodynamic limit, and γ is an exponent. As it is shown in the inset of Fig. 4, it is found that close to the critical edge, A_P vanishes with $\gamma = 4/3$ ($A_\infty \sim 0$) while, far from criticality, one has A_∞ positive with the same value of γ. So, our finite size analysis of the Monte Carlo data allows us to distinguish between the FP and OB regimes in agreement with the mean-field results. Furthermore, we have performed a Fourier analysis of the temporal signals as is shown in Fig. 5. Within the FP regime we observed a pure "1/f" white noise, but crossing to the OB state the spectra shows a peak corresponding to the characteristic frequency of the system $f^* \simeq 3 \times 10^{-2}$ mcs^{-1}. Fourier analysis of time series measured using samples of different size (100 L.U. $\leq L \leq 1000$ L.U.) shows that f^* is independent of L, so it can truly be identified as the natural frequency of the system.

Snapshot configurations of the system within the OB regime are quite different from those characteristic of the FP regime already shown in Fig. 2. In fact, as is shown in Fig. 6, when the density of preys is maximum there is at least a "percolating cluster" of preys spanning the whole lattice [see, e.g., Fig. 6(a)] while small "colonies" of predators are placed almost at random. However, this configuration favors the reproduction of predators that causes the density of preys to decrease [Fig. 6(b)]. Here, small (nonpercolating) clusters of preys are surrounded by predators. So, the OB can be thought as a sequence of alternating percolation events. For details on the percolation theory see, e.g., [16].

In order to perform a quantitative analysis of the transition we have evaluated the percolation probability (P_{pr}) measured for clusters of preys as a function of B_P keeping $D_P = 0.25$, $B_H = 0.5$, and $D_H = 0.99$ as is shown in Fig. 7. Inside the FP regime one has $P_{pr} = 1$ and the population of
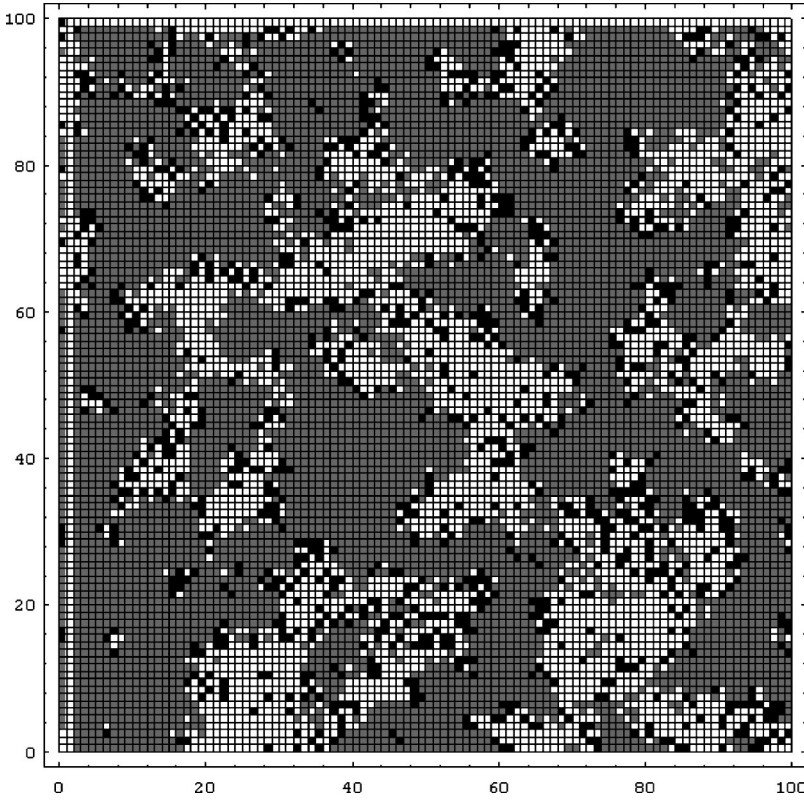
FIG. 3. Snapshot configuration of the system taken within the FP regime for $D_P = 0.25$ and $B_P = 0.45$. Predators are shown as black points and preys are gray. Within this regime the biggest cluster of preys always percolates across both directions of the sample.

both prey and predators is almost constant. However, just at the onset of the OB regime one observes for the first time no-percolating clusters of preys. From Fig. 7 it follows that increasing the lattice size, the P_{pr} vs B_P plots approach a stepped function with a sharp edge close to $B_P \sim 0.5$. In order to determine the critical percolation edge in the thermo-

dynamic limit, let us first define L-dependent thresholds $B_P(L)$ as a fixed point such that $P_{pr}\{B_P(L)\} \equiv$ const. Using this method [16] we have evaluated three sets of L-dependent edges taking three values of the constant, namely, 0.2, 0.4, and 0.6. According to the finite-size scaling theory [16],

$$B_P(L) = B_{P\infty} + ML^{-1/\nu}, \qquad (6)$$

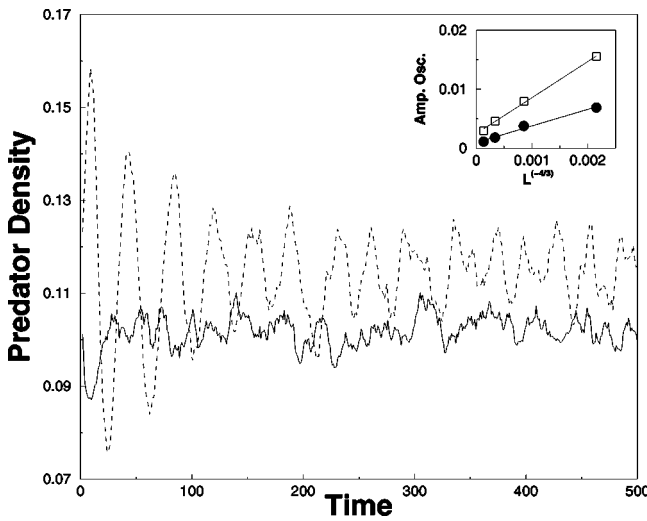where $B_{P\infty}$ is the percolation threshold in the thermodynamic

FIG. 4. Plot of the predator density, measured in unit of number of predators per unit area, versus time, measured in mcs, as obtained from Monte Carlo simulations. ''Full line '' $D_P = 0.25$, $B_P = 0.4$ (noise in the fixed point regime), ''dashed line '' $D_P = 0.25$, $B_P = 0.6$ (oscillatory regime). The inset shows plots of the amplitude of the oscillations of predator density versus $L^{-\gamma}$ ($\gamma = 4/3$), where L is measured in L.U. ● $D_P = 0.25$ and $B_P = 0.4$, □ $D_P = 0.25$ and $B_P = 0.7$.
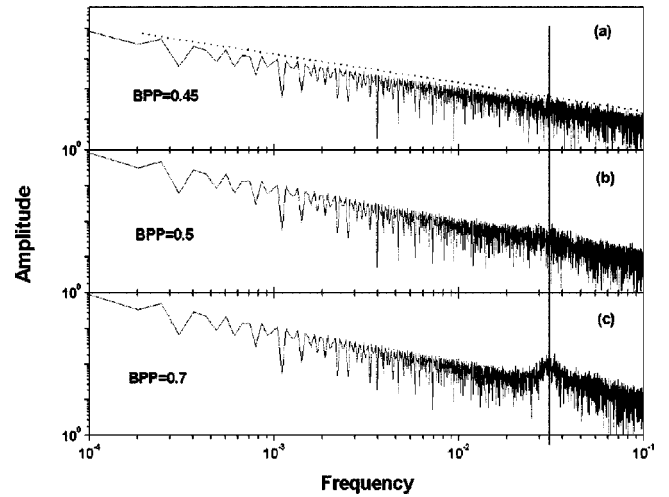

FIG. 5. Fourier spectra of temporal series of the prey density obtained for different values of B_P. The amplitude is measured in arbitrary units and the frequency in mcs^{-1}. The vertical full line shows the location of the natural frequency $f^* \simeq 0.03$ mcs^{-1}. The dashed line in (a) has slope ''-1 ,'' i.e., $1/f$ noise, and has been drawn for the sake of comparison.
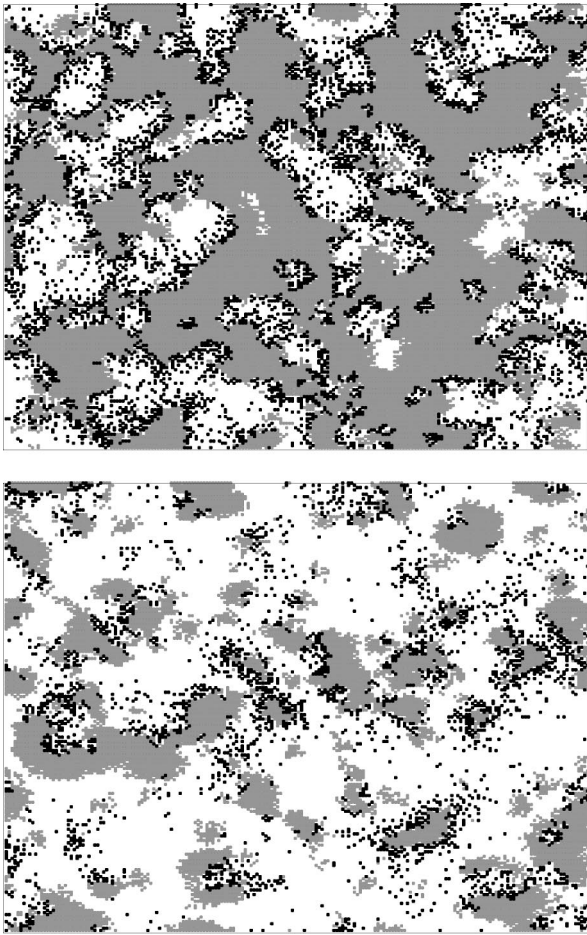
(a)

(b)

FIG. 6. (a) and (b) are snapshot configurations of the system taken within the oscillatory regime. Predators are shown as black points and preys are grey. Notice that (a) and (b) correspond to percolating and nonpercolating stages, respectively. More details in the text.
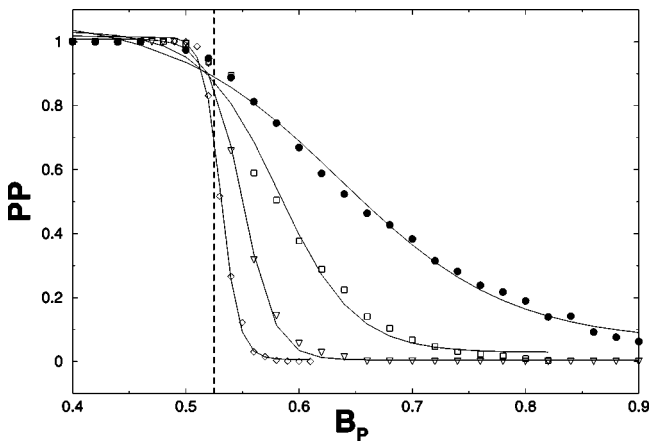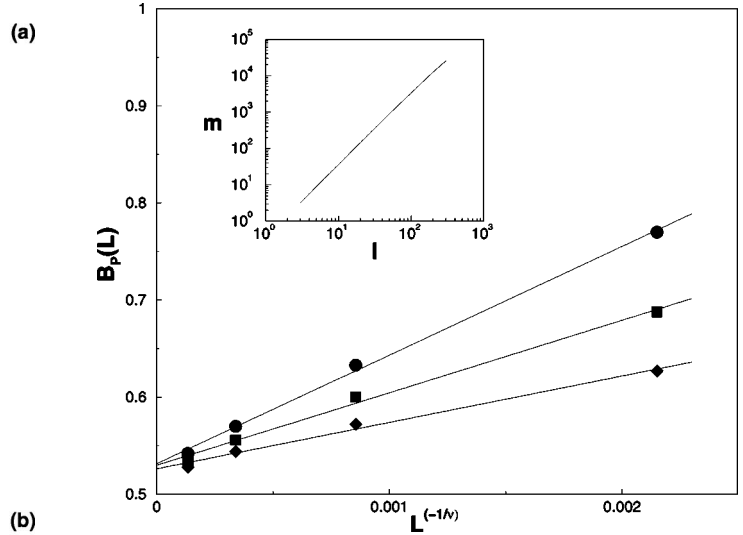

FIG. 8. Plot of the L-dependent critical thresholds $B_P(L)$ versus $L^{-1/\nu}$ with $\nu = 4/3$, where L is measured in LU. Data evaluated at: ● $P_{pr}=0.2$, □ $P_{pr}=0.4$, and ◇ $P_{pr}=0.6$. The inset shows a plot of the number of preys "m" versus "l" —measured in L.U.— obtained at criticality, which gives a straight line with slope $D_F = 1.90$ [see Eq. (7)]. More details in the text.

limit, M is a constant, and ν is the correlation length exponent. The best fit of the data (Fig. 8), which is obtained taking $\nu = \frac{4}{3}$ as in the standard percolation (SP) problem in two dimensions [16], gives $B_{P\infty} \cong 0.525 \pm 0.005$. Just at criticality, prey density is close to $\rho_H \simeq 0.47$. This figure is smaller than the critical occupation probability of the SP model, namely, $p_c \cong 0.59275$, suggesting the existence of "attractive" interactions between preys that may be a consequence of both, the operation of the smart escape rule and the fact that the prey's offsprings are born at nearest-neighbor sites. The fractal dimension of the incipient percolating cluster D_F is given by

$$m \propto l^{D_F}, \qquad (7)$$

where m is the "mass" (number of preys) within a characteristic length l (measured in L.U.). Using the box counting method we obtain $D_F \cong 1.90 \pm 0.02$ (see the inset in Fig. 8) in excellent agreement with the fractal dimension of the SP incipient cluster, namely, $D_F \cong 1.89$ [16]. Considering the scaling relationship [16] $D_F = d - \beta/\nu$, where β is the order parameter critical exponent, we conclude that the percolation transition associated with the FP-OB transition belongs to the same universality class as the SP model.

It should be noticed that our claim of the occurrence of an OB in the thermodynamic limit is in contrast to the conclusions stated by Boccara *et al.* [11] using a similar prey-predator model. In fact, they have found that the oscillatory regime is restricted to finite samples only. The different behavior observed may be due to the fact that Boccara *et al.* [11] have used a cellular automata update rule for the dynamics of coexistence of species while the escape-pursuit dynamics is updated sequentially. In contrast, in the present work both types of dynamics have been performed sequen-

FIG. 7. Plots of the percolation probability (P_{pr}) versus B_P for lattices of different size ● $L=100$ L.U., □ $L=200$ L.U., ▽ $L = 400$ L.U., ◇ $L=800$ L.U. In order to guide the edges, data were fitted using a Boltzmann sigmoid (full line). The dashed line at $B_P = 0.525$ shows the location of the critical edge.

tially. It is known that in some cases both types of updating display essentially the same physical properties, while in other examples, they lead to different results as in the present work.

Finally, it is worth discussing the differences between the present model with smart escape-pursuit rules (SEP) and a simpler one that only considers random diffusion (RD). From the qualitative point of view the major difference arises on the structure of the spatial patterns generated. Let us first consider an epidemic study, suitable for the location of the irreversible transition between prey extinction and coexistence of both species. In this case few predators are released in the center of a lattice fully covered by preys. It is observed that for SEP, the predators tend to form a ring with a well-defined predator-prey interface. The ring propagates outwards keeping empty sites inside it and the interactions between species is favored. In contrast, for RD the ring of predators is much fuzzy and preys can escape crossing it. Consequently, the interface between preys and predators at the expanding ring is not well defined as in the previous case. The probability of predators to catch a prey decreases and the effective probability for the predators to die increases due to smaller reproduction chances. This qualitative picture has quantitative consequences since the location of the extinction-coexistence transition becomes shifted toward larger values of B_P, e.g., we get $B_P^{E\text{-}C} \simeq 0.36$ and $B_P^{E\text{-}C} \simeq 0.38$ for the SEP and the RD cases, respectively. Considering the transition between the FP and the OB states, the observed patterns are consistent with the previous discussion. Compact clusters of preys surrounded by predators are observed for SEP. This configurations favor the prey-predator interaction. However, for RD the interface between clusters of different species is not so well defined and the interaction is less effective. Due to this effect, for the case of RD the onset of the OB takes place at lower values of B_P, e.g., we get $B_P^{FP\text{-}OB} \simeq 0.50$ and $B_P^{FP\text{-}OB} \simeq 0.47$ for the SEP and the RD cases, respectively. Summing up, the overall effect of RD is to reduce the width of the FP regime that occurs in a narrow interval of B_P values. It should also be mentioned that well inside the coexistence regime, the introduction of an error when selecting the escape-pursuit direction generates the onset of spiral patterns that currently are under study [17].

IV. CONCLUSIONS

In summary, we have studied a model of competitive population dynamic. The system displays absorbing states and active regimes. The former can be either nonequilibrium steady states or oscillatory states, respectively. The onset of oscillations at global scale is triggered by a dynamic percolation process. It is worth mentioning that there exist numerous systems that can be described in terms of competitive and cooperative interactions. So, our study is not simply restricted to population dynamics but can be extended to a variety of situations emerging from different scientific fields.

ACKNOWLEDGMENTS

[1] N. Konno, *Phase Transitions on Interacting Particle Systems* (Springer-Verlag, New York, 1985).

[2] A. S. Mikhailov, *Foundations of Synergetics I*, 2nd ed. (Springer-Verlag, Berlin, 1994); A. S. Mikhailov and A. Yu. Loskutov, *Foundations of Synergetics II* (Springer-Verlag, Berlin, 1991).

[3] C. W. Gardiner, *Stochastic Methods* (Springer-Verlag, Berlin, 1983).

[4] A. Czirók *et al.*, Phys. Rev. Lett. **81**, 3038 (1998).

[5] A. Czirók *et al.*, Phys. Rev. E **54**, 1791 (1996).

[6] J. M. Lopez and H. J. Jensen, Phys. Rev. Lett. **81**, 1734 (1998).

[7] T. Vicsek *et al.*, Phys. Rev. Lett. **75**, 1226 (1995); E. Albano, *ibid.* **77**, 2129 (1996); J. Toner and Y. Tu, Phys. Rev. E **58**, 4828 (1998).

[8] A. J. Lotka, Proc. Natl. Acad. Sci. U.S.A. **6**, 410 (1920); A. J. Lotka, *Elements of Physical Biology* (Willams and Wilkins, Baltimore, 1925); V. Volterra, Atti Accad. Naz. Lincei, Cl. Sci. Fis., Mat. Nat., Rend. **6**, 31 (1931).

[9] I. R. Epstein and J. A. Projman, *An Introduction to Nonlinear Chemical Dynamics* (Editorial Oxford University Press, New York, 1998); see, for example, Fig. 1.3.

[10] J. Vilar and R. Solé, Phys. Rev. Lett. **80**, 4099 (1998).

[11] N. Boccara *et al.*, Phys. Rev. E **50**, 4531 (1994).

[12] N. Shimoyama, K. Sugawava, T. Mizugichi, Y. Hahakana, and M. Sano, Phys. Rev. Lett. **76**, 3870 (1996).

[13] Notice that the case $D_P = 0$ is absorbing since predators will ultimately eat all preys.

[14] P. Grassberger and A. de la Torre, Ann. Phys. (N.Y.) **122**, 373 (1979); P. Grasberger, J. Phys. A **22**, 3673 (1989).

[15] For example, the term A is evaluated considering the birth probability of a prey (B_H), the probability of absence of predators in the prey's visual neighborhood $(1 - D_P)^{(2M_P+1)^2-1}$ and the factor $[1 - (\rho_P + \rho_H)^8]$, which is the probability to have "at least" an empty site at the nearest and next-nearest neighbor sites (8 in total, which gives the exponent).

[16] D. Stauffer and A. Aharony, *Introduction to Percolation Theory*, 2nd ed. (Taylor & Francis, London, 1992).

[17] A. F. Rozenfeld, J. L. Gruver, E. V. Albano, and S. Havlin (unpublished).